Proteome adaptations under contrasting soil phosphate regimes of Rhizophagus irregularis engaged in a common mycorrhizal network

Ghislaine Recorbet, Silvia Calabrese, Thierry Balliau, Michel Zivy, Daniel Wipf, Thomas Boller, Pierre-Emmanuel Courty

Proteome adaptations under contrasting soil phosphate regimes of *Rhizophagus irregularis* engaged in a common mycorrhizal network

Ghislaine Recorbet[1], Silvia Calabrese[2], Thierry Balliau[3], Michel Zivy[3], Daniel Wipf[1], Thomas Boller[2], Pierre-Emmanuel Courty[1]

[1]Agrécolologie, AgroSup Dijon, CNRS, Université de Bourgogne, INRAE, Université Bourgogne Franche-Comté, Dijon, France

[2]Department of Environmental Sciences, Botany, Zurich-Basel Plant Science Center, University of Basel, Basel, Switzerland

[3]PAPPSO, GQE - Le Moulon, INRAE, Univ. Paris-Sud, CNRS, AgroParisTech, Univ. Paris-Saclay, 91190 Gif-sur-Yvette, France.

Corresponding author: Ghislaine Recorbet, email:ghislaine.recorbet@inrae.fr

Highlights:

- The ERM of *R. irregularis* was grown between poplar and sorghum under Pi limitation or not
- Shotgun proteomic and qRT-PCR approaches shed light on the ERM adaptive mechanisms to Pi availability
- Lipids are used as the main C source for fungal development in low-Pi condition
- Pi mobilization and N catabolism are stimulated in low-Pi condition

Keywords: mycorrhizal symbiosis, shotgun proteomic, *Rhizophagus irregularis*, extra-radical mycelium, common mycelial network, phosphate nutrition.

Abstract

For many plants, their symbiosis with arbuscular mycorrhizal fungi plays a key role in the acquisition of mineral nutrients such as inorganic phosphate (Pi), in exchange for assimilated carbon. To study gene regulation and function in the symbiotic partners, we and others have used compartmented microcosms in which the extra-radical mycelium (ERM), responsible for mineral nutrient supply for the plants, was separated by fine nylon nets from the associated host roots and could be harvested and analysed in isolation. Here, we used such a model system to perform a quantitative comparative protein profiling of the ERM of *Rhizophagus irregularis* BEG75, forming a common mycorrhizal network (CMN) between poplar and sorghum roots under a long-term high- or low-Pi fertilization regime. Proteins were extracted from the ERM and analysed by liquid chromatography-tandem mass spectrometry.

This workflow identified a total of 1301 proteins, among which 162 displayed a differential amount during Pi limitation, as monitored by spectral counting. Higher abundances were recorded for proteins involved in the mobilization of external Pi, such as secreted acid phosphatase, 3',5'-bisphosphate nucleotidase, and calcium-dependent phosphotriesterase. This was also the case for intracellular phospholipase and lysophospholipases that are involved in the initial degradation of phospholipids from membrane lipids to mobilize internal Pi. In Pi-deficient conditions. The CMN proteome was especially enriched in proteins assigned to beta-oxidation, glyoxylate shunt and gluconeogenesis, indicating that storage lipids rather than carbohydrates are fuelled in ERM as the carbon source to support hyphal growth and energy requirements. The contrasting pattern of expression of AM-specific fatty acid biosynthetic genes between the two plants suggests that in low Pi conditions, fatty acid provision to the fungal network is mediated by sorghum roots but not by poplar. Loss of enzymes involved in arginine synthesis coupled to the mobilization of proteins involved in the breakdown of nitrogen sources such as intercellular purines and amino acids, support the view that ammonium acquisition by host plants through the mycorrhizal pathway may be reduced under low-Pi conditions. This proteomic study highlights the functioning of a CMN in Pi limiting conditions, and provides new perspectives to study plant nutrient acquisition as mediated by arbuscular mycorrhizal fungi.

1. Introduction

Phosphorus (P), as a component of nucleic acids, chemical energy (ATP), cell membrane phospholipids, signal transduction processes, and regulation of enzyme activities, is an essential element for all living organisms. Because P also serves critical roles in photosynthesis, low P availability is a major factor constraining plant growth and metabolism in many soils worldwide. Thus, application of large amounts of Pi fertilizers are used ensure plant productivity in most current agricultural systems (Smith et al. 2011). Crop fertilization has notably tripled the rate of consumption of P, increasing crop production, while in the same time accelerating soil degradation and water eutrophication (Conley et al. 2009). In addition**,** P fertilizers are mainly derived from mined rock phosphate deposits, and these are predicted to become a limiting factor for food production within the next century (van Vuuren et al. 2010).

An alternative to the input of Pi fertilizers is to exploit the mechanisms developed by many P-limited plants to improve P use efficiency in agro-ecosystems, in particular the mutualistic symbiosis with arbuscular mycorrhizal fungi (AMF) of the phylum Glomeromycota (Tedersoo et al. 2018). Approximately 80% of terrestrial plant species engage in this symbiosis, including the majority of agricultural crops (Smith and Read, 2008). AMF benefit crop productivity because of their ecosystem services (Gianinazzi et al. 2010). One prominent function of AMF consists in their contribution to plant Pi acquisition, absorbed from the soil solution through hyphal scavenging of soil volumes that are not accessible by plant roots (Smith et al. 2011). It has been estimated that inoculation with AMF might result in a reduction of approximately 80% of the recommended fertilizer P rates under certain conditions (Jakobsen 1995). In return, AMF are supplied with host organic carbon, in the form of sugar and lipid (Gutjahr and Parniske 2013; Roth and Paszkowski 2017).

In arbuscular mycorrhizal (AM) plants, the extra-radical mycelium (ERM) that develops outside of the host root, is the component of mycorrhiza that mines rhizospheric and bulk soil to acquire scarce nutrients and translocate them to the fungus–root interface where transfer to the host plant is performed (Olsson et al. 2014). Building on the ERM, the AM phosphate pathway involves the uptake of soil Pi at the soil-fungus interface through high-affinity fungal phosphate transporters (PTs) (Garcia et al. 2016; Wang et al. 2017). Pi accumulates in the vacuoles of extraradical hyphae as polyphosphate (polyPi) (Ezawa et al. 2004). PolyPi chains are thought to be transferred by a tubular vacuolar network into the intraradical hyphae and arbuscules (Uetake et al. 2002). Pi is hydrolyzed from polyPi by a fungal phosphatase and exopolyphosphatase, after which the Pi is released into the plant interfacial apoplast of arbuscules (Javot et al. 2007). In this manner, AM fungi give plants access to Pi beyond the depletion zone that develops around the roots.

Despite the key role of the ERM in mineral plant nutrition, current knowledge regarding the global metabolic mechanisms by which the ERM responds to Pi availability remains scarce. Using *Rhizophagus* grown with *Lotus japonicus* under phosphorus-deficient conditions, Kikuchi et al. (2014) reported the induced expression of the genes encoding Pi symporters, P-type ATPases and polyP polymerase four hours after Pi application to Pi-starved hyphae. Howerver, because of the time-dependent outcome of symbiotic relationships in response to nutrient availability (Olsson et al. 2006), it is likely that the metabolism of external hyphae may differ between short- and long-term Pi shortage. In addition, as AM symbionts exhibit a broad host spectrum, ERM can connect the roots of the same or different plant species through the formation of a common mycelial network (CMN), which can transfer nutrients to several plants simultaneously (Walder et al. 2012; Felbaum et al. 2014; Bücking et al. 2016; Calabrese et al. 2019). The ERM provides extensive pathways for nutrient fluxes through the soil and among plants, and its functioning presumably relies on the existence of a complex regulation of fungal metabolism with regard to nutrient sensing, production of specific enzymes, and resource partitioning between host roots and their fungal symbionts (Leake et al. 2004; Walder et al. 2012). Although CMN are known to influence plant establishment/survival, physiology and defence (Gorzelak et al. 2015), information is scarce regarding the characterization of the CMN metabolic adaptations to contrasting Pi fertilization regimes.

In a previous study, when performing metabolome analysis on the ERM of the AMF *Rhizophagus irregularis* associated to *Populus trichocarpa* and *Sorghum bicolor*, we observed that the metabolite profile of the ERM was not significantly affected by Pi availability (Calabrese et al. 2019). However, not only in mammals and plants, but also in fungi, studies over the years have revealed that metabolic pathways are strongly regulated by post-transcriptional control of the proteome, including protein degradation, allosteric changes, and posttranslational modifications, which expand the organism's capacity to respond to nutrient availability (Gutterridge et al. 2010; Plaxton and Tran, 2011; Lan et al. 2012). This is especially true for Pi that acts as an allosteric activator or inhibitor of many enzymes (Gregory et al. 2009). In this regard, proteomics may likely be able to decipher key mycelial metabolic pathways involved in fungal adaptation to differential Pi levels by providing a valuable overview of expression changes of the most abundant proteins in the cell (Alexova and Millar, 2013). Of note, although mass spectrometry (MS) does not provide information about enzyme activity, protein amounts coupled to functional grouping correlate with microbial activity (Wilmes and Bond, 2006; Siggins et al. 2012). With the aim to enhance our understanding of the CMN fungal metabolic pathways as affected by Pi availability, we performed a quantitative comparative protein profiling of the ERM grown

between poplar and sorghum roots under a long-term, high- or low-, Pi fertilization regime. To decipher the fungal proteome, proteins were extracted from the ERM and analysed by liquid chromatography-tandem mass spectrometry (LC-MS/MS). Changes in protein amount between the ERM proteomes obtained under high and low-Pi conditions were further monitored by spectral counting. The biological significance of the Pi-responsive proteins is discussed with special regard to fungal energetic resources and Pi scavenging/recycling strategies.

2. Materials and Methods

2.1. Biological material, microcosms and phosphate fertilization

Experiments were performed as previously described (Calabrese et al. 2019), using *Populus trichocarpa* cuttings (clone 10174, Orléans, France) and *Sorghum bicolor* (L.) Moench, cv Pant-5. After sterilization in 2.5% KClO for 10 min, seeds were germinated in the dark at 25 °C for three days. Microcosms were set-up in tripartite compartments consisting of two root hyphal compartments (1020 ml each) attached to one central hyphal compartment (1100 ml) (**Supplementary Figure 1**). Root hyphal and central compartments were filled with 925 and 1000 g of an autoclaved (120°C, 20 min) quartz sand (Alsace, Kaltenhouse, Trafor AG, Basel): zeolithe (Symbion, Czech Republic) substrate (1:1, w:w), respectively. Poplar cuttings were planted into one of the outside compartments and sorghum seedlings into the other. Both plants were inoculated with *Rhizophagus irregularis*, isolate BEG75 (Inoculum Plus, Dijon, France). For inoculation, plants were supplemented with 1 ml of a spore suspension (110 spores in 1 ml of 0.01 M citrate buffer, pH 6). Compartments were separated by two 21 µM meshes and one 3 mm mesh, to allow the AMF to grow from one compartment to the other but to avoid plant roots protruding into the hyphal compartment. Plants were fertilized once a week with 10 ml Hoagland solution without Pi, until all plants showed signs of phosphate depletion. From the 22nd week, either high-Pi (560 µM) or low-Pi (28 µM) containing Hoagland solution was applied to the middle hyphal compartment for 9 weeks. For each P treatment, the experimental setup was replicated three times. Plants were grown under controlled condition 16 h of light [220 µE m^{-2} s^{-1}] at 25 °C and 8 h of dark at 20 °C, constant relative aerial humidity of 65 %.

2.2. Harvest, mycorrhizal colonization measurements, and P extraction

The ERM was extracted by suspending the substrate of the hyphal compartment with tap water and fishing the hyphae from the surface using a 32 µM mesh. This step was repeated several times. Afterwards, the cleaned ERM samples were snap frozen in liquid nitrogen and stored at -80 °C. Roots from the plant

compartments were removed from substrate under tap water and cut into 1 cm pieces. Samples (about 100mg) were either snap frozen and stored at -80 °C for further gene expression analysis or stored for root colonization measurements. For that purpose**,** roots were immersed in 10% KOH and stored at 4 °C overnight. The next day, the roots were rinsed and immersed in lactic-acid glycerol water (1:1:1, v:v:v) for destaining. Total colonization count was performed using the magnified intersection method (McGonigle et al. 1990). Mycorrhizal parameters were subjected to arcsine square root transformation before comparison of means using Student's *t*-test with a value of $p < 0.05$ considered to be statistically significant.

To determine the total P concentration in poplar and sorghum, root and shoot dried samples were ground using a ball mill. Up to 500mg were used for the modified P extraction method by Murphy and Riley (1962).

2.3. Protein extraction, prefractionation, and digestion

For the two Pi fertilization regimes, protein extraction from frozen ERM (1 to 2g equivalent fresh weight) was performed on three biological replicates using the phenol extraction protocol described by Dumas-Gaudot et al. (2004). Briefly, ERM was ground into liquid nitrogen and homogenised in 10 ml of 0.5 M Tris-HCl, pH 7.5, lysis buffer that contained 0.7 M sucrose, 50 mM EDTA, 0.1 M KCl, 10 mM thiourea, 2 mM PMSF and 2% (v/v) β-mercaptoethanol. One volume of Tris-buffered phenol was added and, after mixing for 30 min, the phenolic phase was separated by centrifugation and rinsed with another 10 ml of lysis buffer. Proteins were precipitated overnight at -20 °C after adding 5 volumes of methanol containing 0.1 M ammonium acetate. The pellet, recovered by centrifugation, was rinsed with cold methanol and acetone and dried under nitrogen gas. Proteins were solubilized in 200 µl of Laemmli buffer (Laemmli et al. 1970) before ultracentrifugation during 30 min (Beckman Airfuge, 30 psi). Protein amount in the supernatant was measured according to the Bradford method (Bradford, 1976).

2.4. Sample pre-fractionation and protein digestion

For each biological replicate ($n = 3$) of the two treatments, fungal proteins (20 µg) were pre-fractionated by a 0.7 cm migration on 12% SDS-PAGE. After Coomassie Brillant Blue staining, each lane was cut into seven slices of equal size (1 mm), washed in distilled water and destained using 100 mM NH_4CO_3 in 50% acetonitrile. A reduction step was performed by addition of 40 µl of 10mM dithiotreitol in 50 mM NH_4HCO_3 for 30 min at 56 °C. The proteins were alkylated by adding 30 µl of 55 mM iodoacetamide in 50 mM NH_4HCO_3 and allowed to

react in the dark at room temperature for 45 min. Gel sections were washed in 50 mM NH_4HCO_3, then ACN, and finally dried for 30 min. In-gel digestion was subsequently performed for 7 h at 37 ºC with 125 ng of modified trypsin (Promega) dissolved in 20% (v/v) methanol and 20 mM NH_4CO_3. Peptides were extracted successively with 0.5% (v/v) TFA and 50% (v/v) ACN and then with pure ACN. Peptide extracts were dried and suspended in 25 µl of 0.05% (v/v) TFA, 0.05% (v/v) HCOOH, and 2% (v/v) ACN.

2.5. Liquid chromatography-tandem mass spectrometry (LC-MS/MS) analysis

Peptide separation was performed using an Ultimate 3000 RSLCnano (Thermo fisher Scientific, Waltham, Massachusetts, USA). Peptides were first desalted using a PepMap100 C18 trap column (5 µm, 100Å, Dionex) with 2% ACN (v/v) and 0.1% HCOOH (v/v) in water for 3min at 15 µl/min. Peptides were further separated on a pepmap100 C18 column (5 µm, 15cm x 75 µm, Dionex). The mobile phase consisted of a gradient of solvents A: 0.1% HCOOH (v/v), 2% ACN (v/v) in water and B: 80% ACN (v/v), 0.1% HCOOH (v/v) in water. Separation was set at a flow rate of 0.3 µl/min using a linear gradient of solvent B from 1 to 32% in 32 min, followed by an increase to 35 % in 2 min and finally to 98% for 3 min. Eluted peptides were analysed with a LTQ-Orbitrap Discovery (Thermo Electron) using a nanoelectrospray interface. Ionization (1.3 kV ionization potential) was performed with a liquid junction and a non-coated capillary probe (10 µm i.d.; New Objective). Peptide ions were analysed using Xcalibur 2.0.7 with the following data-dependent acquisition steps (1) full MS scan (mass to charge ratio (*m/z*) 300-1400, centroid mode in orbitrap), (2) MS/MS (qz = 0.22, activation time = 50 ms, and collision energy = 35%, centroid mode in ion trap). Step 2 was repeated for the three major ions detected in step 1 with a minimal intensity of 500 relative abundance. Dynamic exclusion was set to 30 s.

2.6. Protein identification and quantification

Spectra search was performed against the protein sequences from the *R. irregularis* Gloin1_GeneCatalog_proteins (version 20120510, 30282 entries) downloaded from the server http://genome.jgi.doe.gov/Gloin1/Gloin1 using the X!Tandem software (version 2015.04.01.1) (Langella et al. 2017). Enzymatic cleavage was declared as a trypsin digestion with one possible missed cleavage in first pass. Cysteine carbamidomethylation were set to static, while methionine oxidation, protein n-terminal acetylation with or without excision of methionine, dehydration of N-terminal glutamic acid, deamination of N-terminal glutamine and N-terminal carbamidomethyl-cysteine as possible modifications. Precursor mass precision was set

to 10 ppm with a fragment mass tolerance of 0.5 Da. Identified proteins were filtered and grouped using X!Tandem according to (i) the tolerated presence of at least two peptides with an *E-value* smaller than 0.01 and (ii) a protein *E-value* (calculated as the product of unique peptide *E-values*) smaller than 10^{-5}.

Quantification of proteomic data was achieved by spectral counting using normalized spectral abundance factor (NSAF) analysis (Zybailov et al. 2006). A NSAF value was calculated for each protein in the six replicates (three biological replicates x two conditions). As NSAF represent percentages, all data were arcsine square root-transformed to obtain a distribution of values that could be checked for normality using the Kolmogorov-Smirnov test. For each protein identified, significant differences ($p < 0.05$) between transformed NSAF values originating from low- and high-Pi data sets were analysed using the Welch-test (degrees of freedom = n-1), which is compatible with unequal variances between groups (Staher et al. 2014).

2.7. *In silico* analysis

The number of *trans*-membrane (TM) domains and KOG (euKaryotic Orthologous Groups) functional classification were inferred from the JGI genomic resource for *R. irregularis* (https://mycocosm.jgi.doe.gov/Rhiir2_1/Rhiir2_1.home.html). Prediction of protein subcellular localization was performed using WoLF PSORT (https://www.genscript.com/wolf-psort.html), CELLO (http://cello.life.nctu.edu.tw) and DeepLoc 1.0 (http://www.cbs.dtu.dk/services/DeepLoc/). Secreted proteins were predicted according to the Fungal Secretome and Subcellular Proteome KnowledgeBase 2.1 (FunSecKB2; http://proteomics.ysu.edu/secretomes/fungi2/index.php) after Blastp search. Orthologous sequence search was performed with EnsemblPlants (https://plants.ensembl.org/index.html).

2.8. RNA extraction

Total RNA was extracted from lyophilized extra-radical mycelia (Sánchez-Rodríguez et al. 2008; Calabrese et al. 2017; Calabrese et al. 2019), and frozen plant samples using the RNeasy Plant Mini Kit (Qiagen, Courtaboeuf, France). RNA extracts were DNase treated with the DNA-free™ Kit, DNase Treatment and Removal Reagents (AMBION® by life technologies). Total RNA was quantified with the Qbit RNA BR Assay kit and purity was estimated using the Nanodrop (ND-1000, Witec, Switzerland).

2.9. Reverse transcription and qRT-PCR

231 Complementary DNAs (cDNAs) from three biological replicates were obtained using the
232 iScript™cDNA Synthesis Kit (BIO RAD Laboratories, Paolo Alto, CA, United States), using 200 ng of total
233 RNA per reaction. For quantification a two-step quantitative RT-PCR approach was used. Gene specific primers
234 were designed with Primer-BLAST (https://www.ncbi.nlm.nih.gov/tools/primer-blast) and tested as well in
235 amplify 3.1 (http://engels.genetics.wisc.edu/amplify). Target gene expressions were normalized to the expression
236 of the reference gene translation elongation factor in *R. irregularis*. Quantitative RT-PCRs were run in a 7500
237 real-time PCR system (Roche) using the following settings: 95 °C for 3 min and then 40 cycles of 95 °C for 30 s,
238 60 °C for 1 min and 72 °C for 30 s. The number of replicates comprised three biological and three technical
239 replicates per treatment. Differences in gene expression between applied conditions were tested by either
240 Student's *t*-test or one-way ANOVA using SPSS Statistics, version 22 (IBM, Chicago, USA).
241
242 **3. Results and discussion**
243 **3.1. Mycorrhizal colonization and plant P content**
244 In agreement with previous data (Calabrese et al. 2019), the hyphal colonization and the percentage of
245 vesicles at harvest were not significantly different between low and high P treatments in sorghum and poplar
246 (**Supplementary Figure 2**). However, the relative abundance of arbuscules was significantly enhanced in
247 sorghum roots in the low-P conditions relative to the high-P treatment, thereby supporting the view that
248 mycorrhization sustains P acquisition in sorghum during phosphate limitation (Calabrese et al. 2019).
249 Consistently, the total P content in AM sorghum, which reached 350 µg on average, was similar between the two
250 fertilization regimes, while it was significantly ($p < 0.05$) lower (250 µg) in P-limited AM poplar. To monitor Pi
251 acquisition through the fungal side, we measured in the ERM the expression of the high affinity transporter
252 *RiPT1* that was previously found to be regulated in ERM by external P concentration (Maldonado-Mendoza et
253 al. 2001; Calabrese et al. 2019). As shown in **Supplementary Figure 3**, *RiPT1* was up-regulated by external
254 low-P concentrations in the ERM indicating that *RiPT1* participates in soil Pi uptake in our system.
255
256 **3.2. Comparative proteomics**
257 Fungal proteins were phenol-extracted from three biological replicates for each condition, and analysed
258 using LC-MS/MS after pre-fractionation by SDS-PAGE. Using a an *E-value* smaller than 0.01 per peptide and at
259 least two peptides for correct protein assignment, a total of 1301 non-redundant proteins were identified in the
260 six fractions analysed (two treatments x three biological replicates). These 1301 fungal proteins were sorted in

Supplementary Table 1 with respect to their predicted number of *trans*-membrane (TM) domains and KOG functional classification. As anticipated from the lower abundance of proteins integral to membranes relative to soluble proteins (Vit and Petrak, 2017), proteins with a predicted TM domain (11.4%) were underrepresented in the pool of identified proteins (**Table S1**).

To identify the fungal proteins responsive to Pi availability, we compared the means of NSAF values (n = 3) between low- and high-Pi treatments for each of the 1301 proteins identified in **Table S1**. A total of 162 proteins (12.4%) showed a significant ($p < 0.05$) differential amount between the two conditions. As listed in **Supplementary Table 2**, this repertoire encompassed 108 and 54 fungal proteins, the abundance of which increased and decreased under Pi limitation, respectively. According to the MetaCyc database and the MIPS Functional Catalogue (Ruepp et al. 2004; Caspi et al. 2014), these 162 differentially-accumulated proteins belong to 19 biochemical pathways highlighted as framed bold letters **in Figure 1**, and ten biological processes listed in **Table S2**, respectively. **Figure 2** that displays the quantitative distribution of Pi-responsive protein within MIPS functional categories further indicates that low-Pi fertilization led to an increase in processes related to energetics, protein degradation, metabolism and cell growth, concomitantly to a depletion of proteins involved in protein folding.

One of the prominent fungal metabolic responses observed in the ERM under Pi limitation was the broad activation of energetic pathways, including β-oxidation of fatty acids (FAs) (13 proteins), the mitochondrial electron transport chain (ETC)/ membrane-associated energy conservation mechanisms (13 proteins), the glyoxylate/tricarboxylic acid (TCA) cycle and glycolysis/gluconeogenesis (five proteins each) (**Table S2, Figure 1**). Another obvious feature of low-Pi-responsive fungal proteins was the decreased abundance of 13 proteins mediating protein folding such as chaperones and disulfide isomerases, the depletion of the 26S ubiquitin-proteasome system (six proteins) together with the activation of peptide catabolism (six peptidases) (**Table S2, Figure2**). As regards amino acid biosynthesis upon low-Pi fertilization, **Figure 1** shows a noticeable increased amount of enzymes belonging to the methyl cycle and transsulphuration pathway that contribute to cysteine synthesis from methionine, while there was a concomitant depletion of enzymes involved in arginine biosynthesis (ornithine carbamoyltransferase, arginosuccinate lyase). Pi limitation also led to enhanced amounts of enzymes involved in purine catabolism (five proteins) and phospholipid hydrolysis, including phospholipases and phosphatidyl decarboxylase (**Figure 1**). Finally, a similar trend was observed for metabolic pathways related to the synthesis of cell wall precursors, including chitin and galactomannan, a polymer of mannose and galactose (**Figure 1**).

To further underpin this metabolic reprogramming, we searched the literature for the main AM fungal pathways that have been reported to be transcriptionally regulated with special regard to the data published relative to *R. irregularis* genes responsive to a differential Pi supply (Kikuchi et al. 2014; Vijayakumar et al. 2016; Sugimura and Saito, 2017; Xu et al. 2017). Using the primers listed in **Supplementary Table 3**, the relative transcript levels in hyphae under low- and high-Pi conditions were monitored by quantitative RT-PCR. Results displayed in **Table S3** support higher transcript abundance in low-Pi conditions for fungal genes related to β-oxidation (mitochondrial carnitine-acylcarnitine carrier protein), gluconeogenesis (fructose-1,6-bisphosphatase, phosphoenolpyruvate carboxykinase), glyoxylate shunt (malate synthase, isocitrate lyase), TCA cycle (aconitase), phosphate sensing (phosphoserine phosphatase, SPX domain), and decreased transcription of fungal genes involved in arginine biosynthesis (ornithine carbamoyltransferase OTC/ARG3), and protein folding (chaperone HSP104).

3.3. Hyphal development and mobilization of Pi pools are stimulated by Pi limitation

Under Pi limitation, AM fungal colonization is expected to assist the plant mineral element uptake through the development of extra-radical hyphae that access poorly mobile soil nutrients beyond the depletion zone formed around absorbing roots (Olsson et al. 2002; Olsson et al. 2006). In this study, we identified several low-Pi-responsive proteins that are required for the delivery at of secretory vesicles involved in plasma membrane increase at the growing apex (Wessels, 1993; Levin, 2005; Steinberg, 2007). Data in **Table S2** show that Pi limitation enhanced the abundance of Cdc42 and Sec4, which are involved in the formation of lateral hyphal branches, and membrane traffic coupled to polarized vesicle exocytosis, respectively (Virag et al. 2007; Donovan and Bretscher, 2015). This was also the case for enzymes involved in fungal cell wall construction, including the biosynthesis of chitin and galactomannan (**Figure 1**). In addition to a greater effective surface area for absorbing nutrients, another microbial strategy to improve the acquisition of external P consists of the secretion of proteins that increase the release of Pi from the soil to solution (Richardson and Simpson, 2011; Rai et al. 2013). When searching for secreted proteins as predicted by their extracellular localization according to WoLF PSORT, CELLO, or DeepLoc together with exploring the fungal secretome knowledgebase FunSecKB2, we identified in **Table S2** enhanced amounts under Pi limitation for a tartrate-resistant acid phosphatase type 5, a 3',5'-bisphosphate nucleotidase, and a calcium-dependent phosphotriesterase. These enzymes hydrolyse phosphate esters to mobilize Pi from the soil, the latter being made available for fungal uptake by high-affinity Pi transporters (Hinsinger, 2001; Plaxton and Tran, 2011). Consistently, the expression in the fungal ERM of the

high affinity Pi:H^+ transporter *RiPT1* was enhanced under low-Pi supply relative to high-Pi conditions (**Figure S3**), concomitantly to the induction of the vacuolar transporter chaperone VTC4 (**Table S2**). VTC couples synthesis of polyP to its translocation across the tonoplast, thereby avoiding its toxic accumulation in the cytosol (Gerasimaite et al. 2014). Of note, both VTC4 and phosphoserine phosphatase, which were induced in the fungal proteome in low-Pi conditions (**Table S2**), belong to the ten proteins identified in *R. irregularis* that contain a SPX domain (Ezawa and Saito, 2018), which acts as a sensor for inositol pyrophosphate signalling molecules (Wild et al. 2016).

The low-Pi-responsive proteins identified in **Table S2** pointed to lipid remodelling events in the fungal ERM. Among them was the increased abundance of lysophospholipases that contribute to the initial degradation of phospholipids from membrane lipids. A similar trend was observed for a member of phospholipase D family, which has been implicated in glycerophospholipid catabolism during Pi starvation (Li et al. 2006; Jeong et al. 2017). As previously observed in *Zea mays* roots facing P starvation (Calderon-Vazquez et al. 2008), the protein phosphatidylinositol transfer protein SEC14 shows a decreased abundance in low-Pi conditions (**Table S2**). In yeast, inactivation of SEC14 increases the turnover of the phospholipid phosphatidylcholine (Patton-Vogt et al. 1997). Overall, these results suggest a breakdown of fungal membrane phospholipids upon Pi limitation, which allows internal Pi mobilization, and makes the lipid moiety diacylglycerol available for non-phosphorus-lipid biosynthesis (**Figure 1).** In this context, it has been shown that *R. irregularis* ERM contains glycosylated sterols and glycosylated sphingolipids. As these glycolipids are phosphate-free, they can replace phospholipids in the membranes during P deprivation (Wewer et al. 2014). In this line of reasoning, gene expression profiling of *R. irregularis* in roots of *Lotus japonicus* has also highlighted the repression of fungal glycerophospholipid metabolism when plants were shifted to high-Pi conditions (Vijayakumar et al. 2016).

Collectively, these results indicate that in low-Pi conditions not only external Pi is taken up by an extending ERM, but Pi may be also mobilized from internal pools through phospholipid catabolism

3.4. Lipids are used as the main C source for fungal development under Pi limitation

AMF are obligate biotrophs that depend on the supply of carbon (C) from the host in the form of sugar and lipid (Luginbuehl et al. 2017; McLean et al. 2017; Choi et al. 2018). Extra-radical hyphae are unable to synthesize storage lipids, which are transported from the intra-radical mycelium to the ERM (Pfeffer et al. 1999). Currently, it is believed that the transfer of triacylglycerols (TAG) and glycogen to the ERM would provide the energy required both for active P uptake processes from the soil and the synthesis of new C skeletons needed to

extend the ERM in search of new P resource (Bago et al. 2003; Rich et al. 2017; Roth and Paszkowski 2017). As anticipated by Bago and collaborators (2000) according to ^{13}C labelling experiments and low glycolytic enzyme activities in the ERM of AMF, there was a large body of evidence at the proteome level that storage lipids rather than sugars are fuelled in the ERM as the C source to support hyphal extension under low-Pi conditions.

This conclusion was first drawn from the activation under Pi limitation of the β-oxidation of FAs, as inferred from the increased amount of proteins related to FA activation (long chain acyl-CoA synthetase and ligase, acyl-CoA synthetase), carnitine shuttle (mitochondrial carnitine-acylcarnitine carrier protein), and Lynen's helix (acyl-CoA dehydrogenase, enoyl-CoA hydratase, hydroxyacyl-CoA dehydrogenase, ketoacyl-CoA thiolase) (**Table S2**). Second, after β-oxidation, the final product acetyl-CoA can enter the glyoxylate cycle that, convert lipids into carbohydrates through the enzymes isocitrate lyase and malate synthase in fungal glyoxysomes (Lammers et al. 2001). Consistently, the latter enzyme displayed an enhanced abundance in the fungal ERM upon Pi limitation (**Table S2**). In support of the recruitment of the glyoxylate cycle, there was a depleted amount of isocitrate dehydrogenase (**Table S2**), the inactivation of which is believed to force the C flux toward the glyoxylate shunt (Holms, 1996). Third, after the glyoxylate cycle, its net product, succinate, can be imported into mitochondria by dicarboxylate carriers before being oxidized to fumarate by mitochondrial succinate dehydrogenase that couples the TCA cycle with the ETC (Kunze et al. 2006). The abundance of these proteins was notably higher in low-Pi conditions (**Table S2**). Fourth, the glyoxylate cycle enables cells to utilise FAs to fuel gluconeogenesis, as mirrored in the current study by the increased amount upon Pi limitation of enzymes specific for gluconeogenesis, including phosphoenolpyruvate carboxykinase and fructose-1,6-bisphosphatase (**Table S2**). In agreement with the higher abundance of gluconeogenic enzymes, there was in low-Pi conditions a depleted amount of fructose-2,6-bisphosphatase that generates fructose-2,6-bisphosphate, an allosteric inhibitor of fructose-1,6-bisphosphatase (Benkovic and de Maine, 1982; **Figure 1**). Finally, parallel to gluconeogenesis, there was an increased amount in low-Pi conditions of the trehalose-6-phosphate synthase complex that is connected to glycogen biosynthesis through Glc6P, a potent activator of glycogen synthase (François and Parrou, 2001). Within this line, two glycogenesis enzymes, namely phosphoglucomutase and UDP-glucose pyrophosphorylase, displayed a higher abundance under Pi limitation (**Figure 1**). In support of an enhanced glycogen biosynthesis in response to low-Pi conditions, data listed in **Table S3** include a decreased transcription of the fungal gene encoding glycogen phosphorylase, which catalyses the hydrolysis of glycogen.

One rationale behind the oxidation of FAs as the C source to support hyphal growth in Pi-limited condition is that TAG provide energy twice as much as carbohydrates (Berg et al. 2002). In addition, unlike

glycogen catabolism via glycogenolysis and glycolysis, TAG metabolism through beta-oxidation and gluconeogenesis is coupled to the release of Pi (**Figure 1**). This metabolic route implies that energy provision to the fungal ERM during Pi limitation would depend on TAG import from the intra-radical mycelium and plant monoacylglycerol provision to the fungus (Luginbuehl et al. 2017). To test this scenario in our experimental conditions, we compared between Pi-replete and Pi-starved conditions expression changes in the plant genes *KASI* (β-keto-acyl ACP synthase I), *FatM* (ACP-thioesterase), *RAM2* (glycerol-3-phosphate acyl transferase REDUCED ARBUSCULAR MYCORRHIZA2), and *STR2* (half-size ABC transporter STUNTED ARBUSCULE 2), which form an AM-specific operational unit for lipid biosynthesis and transport in arbuscocytes (Keymer et al. 2017). According to the list of AM-specific lipid biosynthetic/transport genes identified in *Medicago truncatula* (Bravo et al. 2016), we used EnsemblPlants to download the corresponding poplar and sorghum orthologs, a step that retrieved 14 and 15 sequences, respectively (**Table S4**). After profiling their expression in the roots of poplar and sorghum in the two Pi conditions, we observed a contrasting pattern of transcript abundance between the two plants in response to Pi deficiency (**Table S4**). While the mRNA level of genes coding KASI, FATM, and STR2 obviously increased in sorghum roots upon low Pi supply, the transcript abundance of genes coding KASI, FATM and RAM2 conversely decreased in poplar roots in the same condition. This pattern of gene expression strongly suggests that in low Pi conditions, FA provision to the ERM is mediated by sorghum roots but not by poplar. Noteworthy, these results are reminiscent of the asymmetry in the terms of trade observed by Walder et al. (2012) between flax and sorghum connected by a CMN, where contrary to flax, sorghum invested massive amounts of C.

3.5. N catabolism is stimulated by Pi limitation

The current model of N assimilation in AM symbiosis includes the synthesis of arginine in ERM, its transfer to the IRM, where it is broken down to release N for transfer to the host plant (Cruz et al. 2007; Tian et al. 2010; Felbaum et al. 2012). In accordance with the mechanisms of mutual exclusion of anabolism and catabolism of arginine, data in **Table S2** indicate a decreased amount of arginosuccinate lyase and ornithine carbamoyltransferase that are involved in arginine biosynthesis. This occured concomitantly to an increased abundance for the enzymes urease and ornithine aminotransferase (OAT), which use the products of arginine catabolism (Govindarajulu et al. 2005; Funck et al. 2008). Given that ammonium in the ERM inhibits the activity of arginase and urease (Cruz et al. 2007; Bücking and Kafle, 2015), these results not only indicate that arginine is catabolized in the ERM, but also that ammonium acquisition by host plants through the mycorrhizal pathway

411 may be reduced in low-Pi conditions. To investigate this possibility, we monitored in low- and high-Pi
412 conditions using qRT-PCR the transcriptional regulation of the ammonium transporters *PtAMT3.1* and
413 *SbAMT3.1* known to display an AM-specific induction in poplar and sorghum roots, respectively (Koegel et al.
414 2013; Calabrese et al. 2019). Results in **Supplementary Figure 4** show that the induction of *PtAMT3.1* and
415 *SbAMT3.1* was only observed in poplar and sorghum AM roots, respectively. In addition, the lower expression
416 of these transporters in AM roots under low-Pi conditions pointed to a decreased ammonium transfer through the
417 AM pathway in both host plants when facing a long-term Pi shortage. These findings agree with the study of
418 Johnson (2010), who reported that AM symbiosis provides the nutrient (P or N) that is most limiting for the host.
419 They are also reminiscent of what observed during *R. irregularis* spore germination in response to root exudates,
420 during which the recruitment of OAT has been proposed to reflect the mobilization of internal nitrogen stores to
421 meet a higher demand for ammonium due to increased fungal growth (Gachomo et al. 2009).
422 There were additional clues within the low-Pi responsive proteins for the mobilization of intracellular N
423 catabolic enzymes that are required for the utilization of secondary N sources when preferred nitrogen sources
424 such as ammonium, are limiting in filamentous fungi (Marzluf 1993). As regards the utilization of purines, five
425 enzymes involved in purine catabolism, namely AICAR transformylase, 5' nucleotidase, purine nucleoside
426 phosphorylase, urate oxidase and urease, displayed an increased abundance in low-Pi conditions (**Table S2,**
427 **Figure 1**). Of note, similarly to OAT, purine catabolic enzymes require nitrogen derepression. The fungal
428 proteins enriched in low-Pi conditions also included intra-cellular components of the proteasome system, the
429 centre for protein degradation, while there was a depletion of several chaperones involved in protein folding
430 (**Table 1**). This indicates that in low-Pi conditions, proteins enter the degradation machinery rather than the
431 chaperone/repair pathway. We also observed an increase in 20S proteasome levels, in concert with an reduction
432 in 26S proteasome subunits (**Table S2**). As the 26S proteasome degrades proteins in an ATP-dependent reaction,
433 while the 20S proteasome does not so, it has been proposed that increased ration of 20S to 26S proteasomes
434 would allow preservation of protein degradation capacity, while saving energy during nutrient deprivation
435 (Bajorek et al. 2003). The mobilization of internal nitrogen catabolic enzymes that are required for the utilization
436 of secondary nitrogen sources overall supports a higher demand for ammonium due to increased fungal growth.
437 Because finely branched hyphae degenerate within a few days (Bago et al. 1998; de Vries et al. 2009), it can be
438 proposed that during long-term Pi deficiency, cell lysis may be a major reservoir for nitrogen in the fungal CMN.
439 AMF can also release peptidases and proteases into the soil that enable the cleaving of organically bound
440 nitrogen (Bonfante and Genre, 2010; Behie and Bidochka, 2014; Bücking and Kafle, 2015). Data in **Table S2**

highlight two fungal proteins accumulating in low-Pi conditions, a subtilisin-related protease and a peptidase M28, which may fulfil this function according to their predicted extracellular localization.

Taken together, arginine and purine catabolism together with extra- and intra-cellular proteolysis indicate that during long-term Pi deficiency, the fungal ERM uses available nitrogen sources from breakdown of external and internal resources for its own metabolism.

Conclusions

As summarized in **Figure 3**, shotgun proteomic and qRT-PCR approaches add novel aspects to the P_i deficiency responses of an AMF engaged in a common mycorrhizal network. Among them is the mobilization of nitrogen catabolic enzymes that are required for the utilization of secondary nitrogen sources. As regards phosphate, they include the identification of secreted 3',5'-bisphosphate nucleotidase and phosphotriesterase that can hydrolyse phosphate esters to mobilize P from the soil. Likewise, the low-Pi-responsive fungal proteome also indicates that Pi may be mobilized from internal Pi pools through fatty acid breakdown coupled to gluconeogenesis, and phospholipid catabolism. The contrasting pattern of expression of AM-specific fatty acid biosynthetic genes between the two plants suggests that in low Pi conditions, fatty acid provision to the fungal network is mediated by sorghum roots but not by poplar. A relevant future challenge will be to assess the contribution of these pathways to plant Pi acquisition.

Acknowledgments

This project was supported by the Swiss National Science Foundation (Grant n° PZ00P3_136651 to P-EC and n° 127563 to TB). The authors also acknowledge the financial support from the Burgundy Franche-Comté Regional Council and the division of Plant Health and Environment of the French National Institute for Agricultural, Food and Environment (INRAE).

Authors' contributions

P-E. C., S.C., and G.R. carried out the experiments. T.B. and M.Z. performed the mass spectrometry analysis of the samples. G.R. analysed the results and wrote the manuscript with support from all authors. P-E. C., T.B., and D.W. supervised the project.

Declaration of Competing Interest

The authors declare no conflicts of interest.

References

Alexova, R., Millar, A.H., 2013. Proteomics of phosphate use and deprivation in plants. Proteomics 13, 609-623.

Bago, B., Azcon-Aguilar, C., Goulet, A., Piché, Y., 1998. Branched absorbing structures (BAS): a feature of the extraradical mycelium of symbiotic arbuscular mycorrhizal fungi. New Phytol. 139, 375-388.

Bago, B., Pfeffer, P.E;, Abubaker, J., Jun, J., Allen, J.W., Brouillette, J., Douds, D.D., Lammers, P.J., Shachar-Hill, Y., 2003. Carbon export from arbuscular mycorrhizal roots involves the translocation of carbohydrate as well as lipid. Plant Physiol. 131, 1496-507.

Bago, B., Pfeffer, P.E., Shachar-Hill, Y., 2000. Carbon metabolism and transport in arbuscular mycorrhizas. Plant Physiol. 124, 948-958.

Bajorek, M., Finley, D., Glikman, M.H., 2003. Proteasome disassembly and downregulation is correlated with viability during stationary phase. Curr. Biol. 13, 1140-1144.

Behie, S.W., Bidochka, M.J., 2014. Nutrient transfer in plant-fungal symbioses. Trends Plant Sci. 19, 734-740.

Benedetto, A., Magurno, F., Bonfante, P., Lanfranco, L., 2005. Expression profiles of a phosphate transporter gene (*GmosPT*) from the endomycorrhizal fungus *Glomus mosseae*. Mycorrhiza 15, 620-627.

Benkovic, S.J., de Maine, M.M., 1982. Mechanism of action of fructose 1,6-bisphosphatase. Adv. Enzymol. Related Areas Mol. Biol. 53, 45-82.

Berg, J.M., Tymoczko, J.L., Stryer, L., 2002. Triacylglycerols are highly concentrated energy stores, in: Freeman, W.H. (Ed.), Biochemistry. 5th edition. New York, Section 22.1. https://www.ncbi.nlm.nih.gov/books/NBK22369/.

Bonfante, P, Genre, A., 2010. Mechanisms underlying beneficial plant-fungus interactions in mycorrhizal symbiosis. Nat. Comun. 1, 48.

Bradford, M.M., 1976. A rapid and sensitive method for the quantification of microgram quantities of protein utilizing the principle of protein-dye binding. Anal. Biochem. 72, 248-254.

Bravo A.,York, T., Pumplin, N., Mueller, L.A., Harrison, M.J., 2016. Genes conserved for arbuscular mycorrhizal symbiosis identified through phylogenomics.Nat. Plant. 2, 15208.

Bücking, H., Kafle, A., 2015. Role of arbuscular mycorrhizal fungi in the nitrogen uptake of plants: current knowledge and research gaps. Agronomy 5, 587-612.

500 Bücking, H., Mensah, J.A., Fellbaum, C.R., 2016. Common mycorrhizal networks and their effect on the
501 bargaining power of the fungal partner in the arbuscular mycorrhizal symbiosis. Commun. Integr. Biol. 9,
502 e1107684.
503 Calabrese, S., Cuisant, L., Sarazin, A., Niehl, A., Erban, A., Brulé, D., Recorbet, G., Wipf, D., Roux, C., Kopla,
504 J., Boller, T, Courty, P.E., 2019. Imbalanced regulation of fungal nutrient transports accordng to phosphate
505 availability in a symbiocosm formed by poplar, sorghum, and *Rhizophagus irregularis*. Front. Plant Sci. 10,
506 1617.
507 Calabrese, S., Kohler, A., Niehl, A., Veneault-Fourrey, C., Boller, T., Courty, P. E. ,2017. Transcriptome
508 analysis of the *Populus trichocarpa-Rhizophagus irregularis* mycorrhizal symbiosis: Regulation of plant and
509 fungal transportomes under nitrogen starvation. Plant Cell Physiol. 58, 1003-1017.
510 Calderon-Vazquez, C., Ibarra-Laclette, E., Caballero-Perez, J., Herrera-Estrella, L., 2008. Transcript profiling of
511 *Zea mays* roots reveals gene responses to phosphate deficiency at the plant- and species-specific levels. J.
512 Exp. Bot. 59, 2479-2497.
513 Caspi, R., Altman T., Billington, R., Dreher, K., Foerster, H., Fulcher, C.A., Holland, T.A., Keseler, I.M.,
514 Kothari, A., Kubo, A., Krummenacker, M., Latendresse, M., Mueller, L.A., Ong, Q., Paley, S., Subhraveti,
515 P., Weaver, D.S., Weerasinghe, D., Zhang, P., Karp, P.D., 2014. The MetaCyc database of metabolic
516 pathways and enzymes and the BioCyc collection of pathway/genome databases. Nucleic Acids Res. 42,
517 D459–D471.
518 Choi, J., Summers, W., Paszkoski, U., 2018. Mechanisms underlying establishment of arbuscular mycorrhizal
519 symbioses. Annu. Rev. Phytopathol. 56, 135-60.
520 Conley, D.J., Pearl, H.W., Howarth, R.W., Boesch, D.F., Sitzinger, S.P., Havens, K.E., Lancelot, C., Linkens,
521 G.E., 2009. Controlling eutrophication: nitrogen and phosphorus. Science 323, 1014-1015.
522 Cruz, C., Egsgaard, H., Trujillo, C., Ambus, P., Requena, N., Martins-Loução, M.A., Jakobsen, I., 2007.
523 Enzymatic evidence for the key role of arginine in nitrogen translocation by arbuscular mycorrhizal fungi.
524 Plant Physiol. 144, 782-792.
525 de Vries, F.T., Bååth, E., Kuyper, T.W., Bloem, J., 2009. High turnover of fungal hyphae in incubation
526 experiments. FEMS Microbiol. Ecol. 67, 389–396.
527 Donovan, K.W., Bretscher, A., 2015. Tracking individual secretory vesicles during exocytosis reveals an ordered
528 and regulated process. J. Cell Biol. 210, 181-189.

Dumas-Gaudot, E., Valot, B., Bestel-Corre, G., Recorbet, G., St-Arnaud, M., Dieu, M., Raes, M., Saravanan, R.S., Gianinazzi, S., 2004. Proteomics as a way to identify extra-radicular fungal proteins from *Glomus intraradices*-RiT-DNA carrot root mycorrhizas. FEMS Microbiol. Ecol. 48, 401-411.

Ezawa, T., Cavagnaro, T.R., Smith, S.E., Smith, F.A., Ohtomo, R., 2004. Rapid accumulation of polyphosphate in extra-radical hyphae of an arbuscular mycorrhizal fungus as revealed by histochemistry and a polyphosphate kinase/luciferase system. New Phytol. 161, 387–392.

Ezawa, T., Saito, K., 2018. How do arbuscular mycorrhizal fungi handle phosphate? New insight into fine-tuning of phosphate metabolism. New Phytol. 220, 1116-1121.

Fellbaum, C.R., Gachomo, E.W., Beesetty, Y., Choudary, S., Strahan, G.D., Pfeffer, P.E., Kiers, E.T., Bücking, H., 2012. Carbon availability triggers fungal nitrogen uptake and transport in arbuscular mycorrhizal symbiosis. P. Natl. Acad. Sci. USA. 109, 2666-2671.

Fellbaum, C.R., Mensah, J.A., Cloos, A.J., Strahan, G.E., Pfeffer, P.E., Kiers, E.T., Bücking, H., 2014. Fungal nutrient allocation in common mycorrhizal networks is regulated by the carbon source strength of individual host plants. New Phytol. 203, 646–656.

François, J., Parrou, J.L., 2001. Reserve carbohydrates metabolism in the yeast *Saccharomyces cerevisiae*. FEMS Microbiol. Rev. 25, 125-45.

Funck, D., Stadelhofer, B., Koch, W., 2008. Ornithine-δ-aminotransferase is essential for arginine catabolism but not for proline biosynthesis. BMC Plant Biology 8, 40.

Gachomo, E., Allen, J.W., Pfeffer, P.E., Govindarajulu, M., Douds, D.D., Jin, H., Nagahashi, G., Lammers, P.J., Shachar-Hill Y., Bücking, H., 2009. Germinating spores of *Glomus intraradices* can use internal and exogenous nitrogen sources for de novo biosynthesis of amino acids. New Phytol. 184, 399-411.

Garcia, K., Doidy, J., Zimmermann, S., Wipf, D., Courty, P.-E., 2016. Take a trip through the plant and fungal transportome of mycorrhiza. Trends Plant Sci. 21, 937-950.

Gerasimaite, R., Sharma, S., Desfougères, Y., Schmidt, A., Mayer, A., 2014. Coupled synthesis and translocation restrains polyphosphate to acidocalcisome-like vacuoles and prevents its toxicity. J. Cell Sci. 127, 5093-5104.

Gianinazzi, S., Gollotte, A., Binet, M.N., van Tuinen, D., Redecker, D., Wipf, D. 2010. Agroecology: the key role of arbuscular mycorrhizas in ecosystem services. Mycorrhiza 20, 519–530.

Gorzelak, M.A., Asay, A.K., Pickles, B.J., Simard, S.W., 2015. Inter-plant communication through mycorrhizal networks mediates complex adaptive behaviour in plant communities. AoB Plants 7, plv050.

559 Govindarajulu, M., Pfeffer, P.E., Abubaker, J., Douds, D.D., Allen, J.W., Bücking, H., Lammers, P.J., Shachar
560 Hill, Y., 2005. Nitrogen transfer in the arbuscular mycorrhizal symbiosis. Nature 435, 819-823.
561 Gregory, A.L., Hurley, B.A., Tran, H.T., Valentine, A.J., She, Y.M., Knowles, V.L., Plaxton, W.C., 2009. *In*
562 *vivo* regulatory phosphorylation of the phosphoenolpyruvate carboxylase AtPPC1 in phosphate-starved
563 *Arabidopsis thaliana*. Biochem. J. 420, 57–65.
564 Gutjahr, C., Parniske, M., 2013. Cell and developmental biology of arbuscular mycorrhiza symbiosis. Ann. Rev.
565 Cell Dev. Biol. 29, 593–617.
566 Gutteridge, A., Pir, P., Castrillo, J.I., Charles, P.D., Lilley, K.S., Oliver, S.G., 2010. Nutrient control of
567 eukaryote cell growth: a systems biology study in yeast. BMC Biol. 8, 68.
568 Hinsinger, P., 2001. Bioavailability of soil inorganic P in the rhizosphere as affected by root-induced chemical
569 changes: a review. Plant Soil 237, 173-195.
570 Holms, H., 1996. Flux analysis and control of the central metabolic pathways in *Escherichia coli*. FEMS
571 Microbiol Rev. 19, 85-116.
572 Jakobsen, I., 1995. Transport of phosphorus and carbon in VA mycorrhizas, in Varma, A., Hock, B. (Eds.),
573 Mycorrhiza. Springer, Berlin, pp. 297-324.
574 Javot, H., Pumplin, N., Harrison, M.J., 2007. Phosphate in the arbuscular mycorrhizal symbiosis: transport
575 properties and regulatory roles. Plant Cell Environ. 30, 310-322.
576 Jeong, K., Baten, A., Waters, D.L., Pantoja, O., Julia, C.C., Wissuwa, M., Heuer, S., Kretzschmar, T., Rose, T.J.,
577 2017. Phosphorus remobilization from rice flag leaves during grain filling: an RNA-seq study. Plant
578 Biotechnol. J. 15, 15-26.
579 Johnson, N.C., 2010. Resource stoichiometry elucidates the structure and function of arbuscular mycorrhizas
580 across scales. New Phytol. 185, 631–647.
581 Keymer, A., Pimprikar, P., Wewer, V., Huber, C., Brands, M., Bucerius, S.L., Delaux, P.M., Klingl, V.,
582 Röpenack-Lahaye, E.V., Wang, T.L., Eisenreich, W., Dörmann, P., Parniske, M., Gutjahr, C., 2017. Lipid
583 transfer from plants to arbuscular mycorrhiza fungi. Elife. 6, e29107.
584 Kikuchi, Y., Hijikata, N., Yokoyama, K., Ohtomo, R., Handa, Y., Kawaguchi, M., Saito, K., Ezawa, T., 2014.
585 Polyphosphate accumulation is driven by transcriptome alterations that lead to near-synchronous and near-
586 equivalent uptake of inorganic cations in an arbuscular mycorrhizal fungus. New Phytol. 204, 638-649.
587 Koegel, S., Boller, T., Lehmann, M.F., Wiemken, A., Courty, P.E., 2013. Rapid nitrogen transfer in the *Sorghum*
588 *bicolor-Glomus mosseae* arbuscular mycorrhizal symbiosis. Plant Signal. Behav. 8, 8.

589 Kunze, M., Pracharoenwattana, I., Smith, S.M., Hartig, A., 2006. A central role for the peroxisomal membrane
590 in glyoxylate cycle function. Biochim. Biophys. Acta 1763, 1441-1452.
591 Laemmli, U.K., Amos, L.A., Klug, A., 1970. Correlation between structural transformation and cleavage of the
592 major head protein of T4 bacteriophage. Cell 7, 191-203.
593 Lammers, P., Jun, J., Abubaker, J., Arreola, R., Gopalan, A., Bago, B., Hernández-Sebastiá, C., Allen, J.W.,
594 Douds, D.D., Pfeffer, P.E., Shachar-Hill, Y., 2001.The glyoxylate cycle in an arbuscular mycorrhizal fungus.
595 Carbon flux and gene expression. Plant Physiol. 127, 1287-1298.
596 Lan, P., Li, W., Schmidt, W., 2012. Complementary proteome and transcriptome profiling in phosphate-deficient
597 Arabidopsis roots reveals multiple levels of gene regulation. Mol. Cell Proteomics 11, 1156-1166.
598 Langella, O., Valot, B., Balliau, T., Blein-Nicolas, M., Bonhomme, L., Zivy, M., 2017. X!TandemPipeline: A
599 tool to manage sequence redundancy for protein inference and phosphosite identification. J. Proteome Res. 2,
600 494-503.
601 Leake, J., Johnson, D., Donnelly, D., Muckle, G., Boddy, L., Read, D., 2004. Networks of power and influence:
602 the role of mycorrhizal mycelium in controlling plant communities and agroecosystem functioning. Can. J.
603 Bot. 82**,** 1016-1045.
604 Levin, DE., 2005. Cell wall integrity signaling in *Saccharomyces cerevisiae*. Microbiol. Mol. Biol. Rev. 69, 262-
605 291.
606 Li, M., Welti, R., Wang, X., 2006. Quantitative profiling of arabidopsis polar glycerolipids in response to
607 phosphorus starvation. Roles of phospholipases D*ζ1* and D*ζ2* in phosphatidylcholine hydrolysis and
608 digalactosyldiacylglycerol accumulation in phosphorus-starved plants. Plant Physiol. 142, 750-761.
609 Luginbuehl, L.H., Menard, G.N., Kurup, S., van Erp, H., Radhakrishnan, G.V., Breakspear, A., Oldroyd, G.E.,
610 Eastmond, P.J., 2017. Fatty acids in arbuscular mycorrhizal fungi are synthesized by the host plant. Science.
611 356, 1175-1178.
612 Maldonado-Mendoza, I.E., Dewbre, G.R., Harrison, M.J., 2001. A phosphate transporter gene from the extra-
613 radical mycelium of an arbuscular mycorrhizal fungus *Glomus intraradices* is regulated in response to
614 phosphate in the environment. Mol. Plant Microbe Interact. 14, 1140–1148.
615 McLean, A.M., Bravo, A., Harrison, M.J., 2017. Plant signaling and metabolic pathways enabling arbuscular
616 mycorrhizal symbiosis. Plant Cell 29, 2319-2335.

McGonigle T. P., Miller M. H., Evans D. G., Fairchild G. L., Swan J. A. (1990). A new method which gives an objective measure of colonization of roots by vesicular—arbuscular mycorrhizal fungi. New Phytol. 115, 495-501.

Marzluf, G.A., 1993. Regulation of sulfur and nitrogen metabolism in filamentous fungi. Ann Rev. Microbiol. 47, 31-55.

Murphy, J., Riley, J.P., 1962. A modified single solution method for the determination of phosphate in natural waters. Anal. Chim. Acta 27, 31-36.

Olsson, O., Olsson, P.A., Hammer, E.C., 2014. Phosphorus and carbon availability regulate structural composition and complexity of AM fungal mycelium. Mycorrhiza 24, 443-451.

Olsson, P.A., Hansson, M.C., Burleigh, S.H., 2006. Effect of P availability on temporal dynamics of carbon allocation and *Glomus intraradices* high-affinity P transporter gene induction in arbuscular mycorrhiza. Appl. Environ. Microbiol. 72, 4115-4120.

Olsson, P.A., van Aarle, I.M., Allaway, W.G., Ashford, A.E., Rouhier, H., 2002. Phosphorus effects on metabolic processes in monoxenic arbuscular mycorrhiza cultures. Plant Physiol. 130, 1162-1171.

Patton-Vogt, J..L, Griac, P., Sreenivas, A., Bruno, V., Dowd, S., Swede, M.J., Henry, S.A., 1997. Role of the yeast phosphatidylinositol/phosphatidylcholine transfer protein (Sec14p) in phosphatidylcholine turnover and INO1 regulation. J. Biol. Chem. 272, 20873-20883.

Pfeffer, P.E., Douds, D.D., Bécard, G., Shachar-Hill, Y., 1999. Carbon uptake and the metabolism and transport of lipids in an arbuscular mycorrhiza. Plant Physiol. 120, 587-598.

Plaxton, W.C., Tran, H.T., 2011. Metabolic adaptations of phosphate-starved plants. Plant Physiol. 156, 1006-1015.

Rai, A, Rai, S, Rakshit, A., 2013. Mycorrhiza-mediated phosphorus use efficiency in plants. Environ. Exp. Biol. 11, 107-117.

Rich, M.K., Nouri, E., Courty, P.E., Reinhardt, D., 2017. Diet of Arbuscular Mycorrhizal Fungi: Bread and Butter? Trends Plant Sci. 22, 652-660.

Richardson, A.E., Simpson, R.J., 2011. Soil microorganisms mediating phosphorus availability update on microbial phosphorus. Plant Physiol. 156, 997-1005.

Roth, R., Paszkowski, U., 2017. Plant carbon nourishment of arbuscular mycorrhizal fungi. Curr. Opin. Plant Biol. 39, 50-56.

Ruepp, A., Zollner, A., Maier, D., Albermann, K., Hani, J., Mokrejs, M., Tetko, I., Güldener, U., Mannhaupt, G., Münsterkötter, M., Mewes, H.W., 2004. The FunCat, a functional annotation scheme for systematic classification of proteins from whole genomes. Nucleic Acids Res. 14, 5539-5545.

Sánchez-Rodríguez, A., Portal, O., Rojas, L. E., Ocaña, B., Mendoza, M., Acosta, M., Jiménez, E., Höfte, M., 2008. An efficient method for the extraction of high-quality fungal total RNA to study the *Mycosphaerella fijiensis-Musa* spp. Interaction.Mol Biotechnol. 40, 299-305.

Siggins, A., Gunnigle, E., Smith, F.A., 2012. Exploring mixed microbial community functioning: recent advances in metaproteomics. FEMS Microbiol. Ecol. 80, 265-280.

Smith, S.E., Jakobsen, I., Grønlund, M., Smith, F.A., 2011. Roles of arbuscular mycorrhizas in plant phosphorus nutrition: interactions between pathways of phosphorus uptake in arbuscular mycorrhizal roots have important implications for understanding and manipulating plant phosphorus acquisition. Plant Physiol. 156, 1050-1057.

Smith, S.E., Read, D.J., 2008. Mycorrhizal symbiosis, third ed. Academic Press and Elsevier, London.

Staehr, P., Löttgert, T., Christmann, A., Krueger, S., Rosar, C., Rolčík, J., Novák, O., Strnad, M., Bell, K., Weber, A.P., Flügge, U.I., Häusler, R.E., 2014. Reticulate leaves and stunted roots are independent phenotypes pointing at opposite roles of the phosphoenolpyruvate/phosphate translocator defective in *cue1* in the plastids of both organs. Front. Plant Sci. 5, 126.

Steinberg, G., 2007. Hyphal growth: a tale of motors, lipids, and the Spitzenkörper. Eukaryot. Cell 6, 351-360.

Sugimura, Y., Saito, K., 2017. Transcriptional profiling of arbuscular mycorrhizal roots exposed to high levels of phosphate reveals the repression of cell cycle-related genes and secreted protein genes in *Rhizophagus irregularis*. Mycorrhiza 27, 139-146.

Tedersoo, L., Sánchez-Ramírez, S., Kõljalg, U., Bahram, M., Döring, M., Schigel, D., May, T., Ryberg, M., Abarenkov, K., 2018. High-level classification of the Fungi and a tool for evolutionary ecological analyzes. Fungal Divers. 90, 135-159.

Tian, C., Kasiborski, B., Koul, R., Lammers, P.J., Bücking, H., Shachar-Hill, Y., 2010. Regulation of the nitrogen transfer pathway in the arbuscular mycorrhizal symbiosis: Gene characterization and the coordination of expression with nitrogen flux. Plant Physiol. 153, 1175-1187.

Uetake, Y., Kojima, T., Ezawa, T. and Saito, M. 2002, Extensive tubular vacuole system in an arbuscular mycorrhizal fungus, *Gigaspora margarita*. New Phytologist 154: 761-768.

van Vuuren, D.P., Bouwman, A.F., Beusen, A.H.W., 2010. Phosphorus demand for the 1970–2100 period: A scenario analysis of resource depletion. Global Environ. Change 20, 428-439.

Vijayakumar, V., Liebisch, G., Buer, B., Xue, L., Gerlach, N., Blau, S., Schmitz, J., Bucher, M., 2016. Integrated multi-omics analysis supports role of lysophosphatidylcholine and related glycerophospholipids in the *Lotus japonicus–Glomus intraradices* mycorrhizal symbiosis. Plant Cell Environ. 39, 393–415.

Virag, A., Lee, M.P., Si, H., Harris, S.D., 2007. Regulation of hyphal morphogenesis by *cdc42* and *rac1*homologues in *Aspergillus nidulans*. Mol. Microbiol. 66, 1579-1596.

Vit, O., Petrak, J., 2017. Integral membrane proteins in proteomics. How to break open the black box? J. Proteomics 153, 8-20.

Walder, F., Niemann, H., Natarajan, M., Lehmann, M.F., Boller, T., Wiemken, A., 2012. Mycorrhizal networks: common goods of plants shared under unequal terms of trade. Plant Physiol. 159, 789-797.

Wang, W., Shi, J., Xie, Q., Jiang, Y., Yu, N., Wang, E., 2017. Nutrient exchange and regulation in arbuscular mycorrhizal symbiosis. Mol. Plant 10, 1147-1158.

Wewer, V., Brands, M., Dörmann, P., 2014. Fatty acid synthesis and lipid metabolism in the obligate biotrophic fungus *Rhizophagus irregularis* during mycorrhization of *Lotus japonicus*. Plant J. 79, 398-412.

Wild, R., Gerasimaite., R, Jung, J.Y., Truffault, V., Pavlovic, I., Schmidt, A., Saiardi, A., Jessen, H.J., Poirier, Y., Hothorn, M., Mayer, A., 2016. Control of eukaryotic phosphate homeostasis by inositol polyphosphate sensor domains. Science 352, 986-990.

Wessels, J.G.H., 1993. Wall growth, protein excretion and morphogenesis in fungi. New Phytol. 132, 397-413.

Wilmes, P., Bond, P.L., 2006. Metaproteomics: studying functional gene expression in microbial ecosystems. Trends Microbiol. 14, 92-97.

Xu, L.J., Jiang, X.L., Hao, Z.P., Li, T., Wu, Z.X., Chen, B.D., 2017. Arbuscular mycorrhiza improves plant adaptation to phosphorus deficiency through regulating the expression of genes relevant to carbon and phosphorus metabolism. Chinese J. Plant Ecol. 41, 815-825.

Zybailov, B., Mosley, A.L., Sardiu, M., Coleman, M.K., Florens, L., Washburn, M.P., 2006. Statistical analysis of membrane proteome expression changes in *Saccharomyces cerevisiae*. J. Proteome Res. 5, 2339-2347.

Figure legends

Figure 1. Schematic overview of the fungal metabolic pathways responsive to low-Pi fertilization, as predicted by spectral counting**.** Metabolic pathways, as inferred from MetaCyc, are indicated in framed bold letters. Red

and green colours refer to increased and decreased protein amounts, respectively. Yellow arrow indicates allosteric inhibition, while blue arrow indicates allosteric activation. ACOX, acyl-coenzyme A oxidase; AICAR, aminoimidazole carboxamide ribotide; CoA, coenzyme A; DAH7P, 3-deoxy-D-arabino-heptulosonate 7-phosphate; DHAP, dihydroxyacetone phosphate; ERM, extra-radical mycelium; ETC, electron transport chain; FA, fatty acid; FOX2, bifunctional hydroxyacyl-CoA dehydrogenase/enoyl-CoA hydratase; GPX, glutathione peroxidase; GSH, reduced glutathione; GST, glutathione S-transferase; H_2O_2, hydrogen peroxide; H_2S, hydrogen sulfide; IMP, inosine monophosphate; IRM, intra-radical mycelium; NADPH, nicotinamide adenine dinucleotide phosphate; P, phosphate; PA, phosphatidic acid; PCM1, phosphoacetylglucosamine mutase; Pi, inorganic phosphate; PPi, inorganic pyrophosphate; PPP, pentose phosphate pathway; PSD, phosphatidylserine decarboxylase; SAM, S-adonesylmethionine; SH, sulfhydryl; SSG, glutathione disulfide; TAG, triacylglycerol; TCA, tricarboxylic acid; UDP, uridine diphosphate; UPS, ubiquitin-proteasome system; UQ, ubiquinone; UQH_2, ubiquinol

Figure 2. Functional distribution of the fungal proteins that display significantly different NSAF values when comparing low- and high-Pi fertilization regimes, as listed in Table2. Bars refer to the number of proteins per functional category, which show either an increased (dark colour) or a decreased (grey colour) NSAF value in low-Pi conditions. Only biological processes accounting for more than 5% of the 162 Pi-responsive proteins identified in Table S2 are presented.

Figure 3. Overview of the metabolic pathways responsive to low-Pi fertilization, as inferred from shotgun proteomic and qRT-PCR approaches. Red and green colours refer to increased and decreased protein and transcript (*) abundance, respectively. AAs, amino acids; Acetyl-ACP, acetyl-acyl carrier protein; ERM, extra-radical mycelium; ETC, electron transport chain; FA, fatty acid; FatM, ACP-thioesterase; IRM, intra-radical mycelium; KASI, β-keto-acyl ACP synthase I; MAG, monoacylglycerol; OAA, oxaloacetate; RAM2, glycerol-3-phosphate acyl transferase REDUCED ARBUSCULAR MYCORRHIZA 2; STR2, half-size ABC transporter STUNTED ARBUSCULE 2; TAG, triacylglycerol; TCA, tricarboxylic acid ;VTC, vacuolar transporter chaperone.

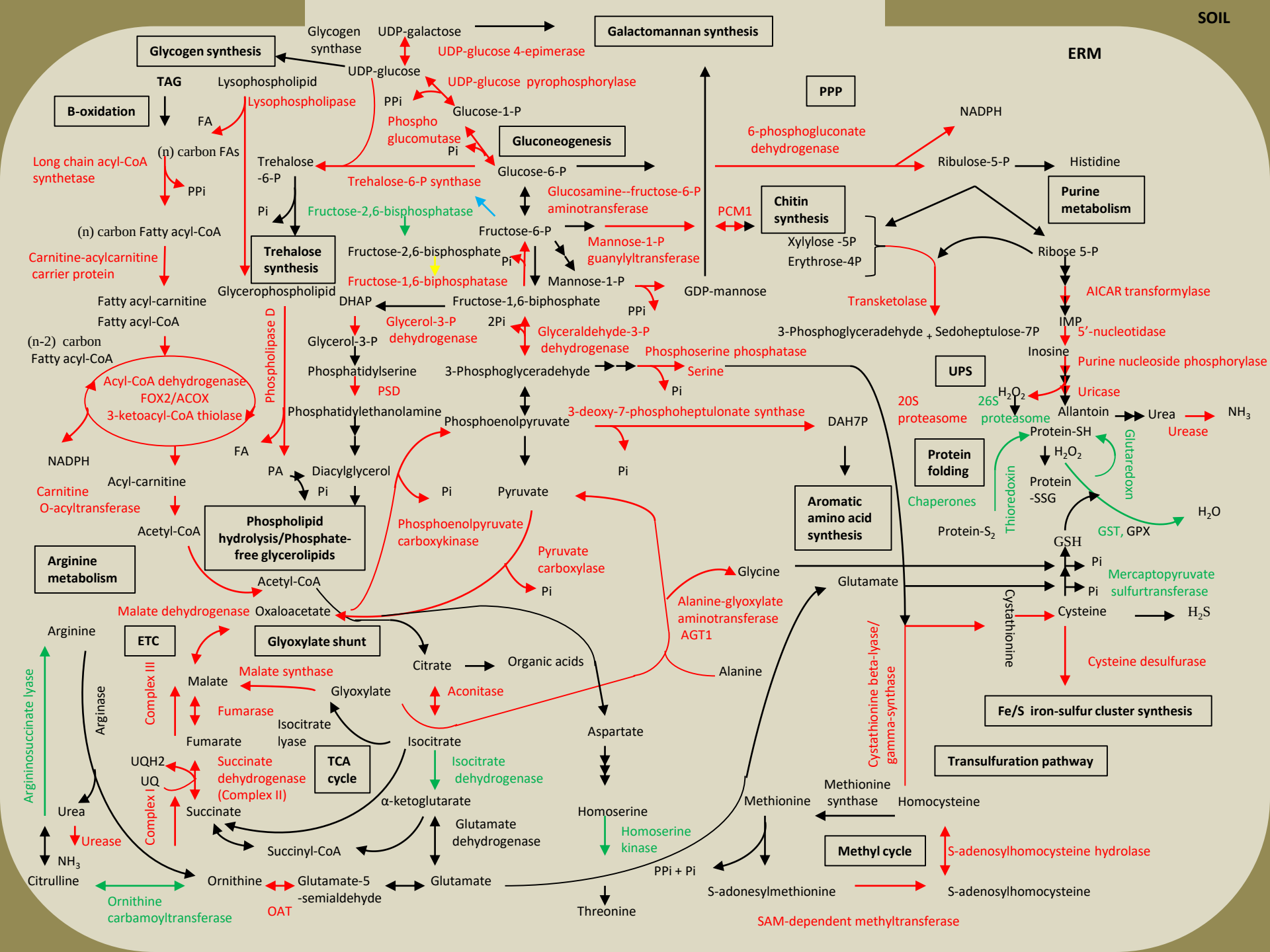
SOIL
ERM
Glycogen synthase
UDP-galactose
Galactomannan synthesis
Glycogen synthesis
UDP-glucose 4-epimerase
UDP-glucose
UDP-glucose pyrophosphorylase
TAG
Lysophospholipid
PPi
Glucose-1-P
B-oxidation
Lysophospholipase
FA
Phospho glucomutase
Pi
Gluconeogenesis
(n) carbon FAs
Trehalose -6-P
Glucose-6-P
Long chain acyl-CoA synthetase
PPi
Trehalose-6-P synthase
Glucosamine--fructose-6-P aminotransferase
Pi
Fructose-2,6-bisphosphatase
Fructose-6-P
PCM1
Chitin synthesis
(n) carbon Fatty acyl-CoA
Trehalose synthesis
Fructose-2,6-bisphosphate
Pi
Mannose-1-P guanylyltransferase
Carnitine-acylcarnitine carrier protein
Fructose-1,6-biphosphatase
Mannose-1-P
Glycerophospholipid
DHAP
Fructose-1,6-biphosphate
GDP-mannose
PPi
Fatty acyl-carnitine
Fatty acyl-CoA
Glycerol-3-P dehydrogenase
2Pi
Glyceraldehyde-3-P dehydrogenase
Phosphoserine phosphatase
(n-2) carbon Fatty acyl-CoA
Glycerol-3-P
Phosphatidylserine
3-Phosphoglyceradehyde
Serine
Pi
Acyl-CoA dehydrogenase FOX2/ACOX 3-ketoacyl-CoA thiolase
Phospholipase D
PSD
Phosphatidylethanolamine
Phosphoenolpyruvate
3-deoxy-7-phosphoheptulonate synthase
DAH7P
NADPH
FA
PA
Diacylglycerol
Pi
Pyruvate
Pi
Acyl-carnitine
Carnitine O-acyltransferase
Phospholipid hydrolysis/Phosphate-free glycerolipids
Aromatic amino acid synthesis
Acetyl-CoA
Phosphoenolpyruvate carboxykinase
Pyruvate carboxylase
Pi
Arginine metabolism
Acetyl-CoA
Glycine
Glutamate
Malate dehydrogenase
Oxaloacetate
Alanine-glyoxylate aminotransferase AGT1
Alanine
Arginine
ETC
Glyoxylate shunt
Citrate
Organic acids
Malate synthase
Malate
Glyoxylate
Aconitase
Complex III
Fumarase
Fumarate
Isocitrate lyase
Isocitrate
Aspartate
UQH2
UQ
Succinate dehydrogenase (Complex II)
TCA cycle
Isocitrate dehydrogenase
Argininosuccinate lyase
Arginase
Complex I
Urea
Succinate
α-ketoglutarate
Homoserine
Urease
Glutamate dehydrogenase
Homoserine kinase
NH3
Succinyl-CoA
Methionine
Methionine synthase
Homocysteine
Citrulline
Ornithine
Glutamate-5 -semialdehyde
Glutamate
PPi + Pi
Methyl cycle
S-adenosylhomocysteine hydrolase
Ornithine carbamoyltransferase
OAT
Threonine
S-adonesylmethionine
S-adenosylhomocysteine
SAM-dependent methyltransferase
Cystathionine beta-lyase/ gamma-synthase
Cystathionine
Cysteine
Cysteine desulfurase
Transulfuration pathway
Fe/S iron-sulfur cluster synthesis
Mercaptopyruvate sulfurtransferase
H2S
PPP
NADPH
6-phosphogluconate dehydrogenase
Ribulose-5-P
Histidine
Purine metabolism
Xylylose -5P
Erythrose-4P
Ribose 5-P
AICAR transformylase
Transketolase
IMP
5'-nucleotidase
3-Phosphoglyceradehyde + Sedoheptulose-7P
Inosine
Purine nucleoside phosphorylase
UPS
Uricase
H2O2
20S proteasome
26S proteasome
Allantoin
Urea
NH3
Urease
Protein folding
Protein-SH
H2O2
Glutaredoxn
Protein -SSG
Chaperones
Thioredoxin
Protein-S2
GSH
GST, GPX
H2O

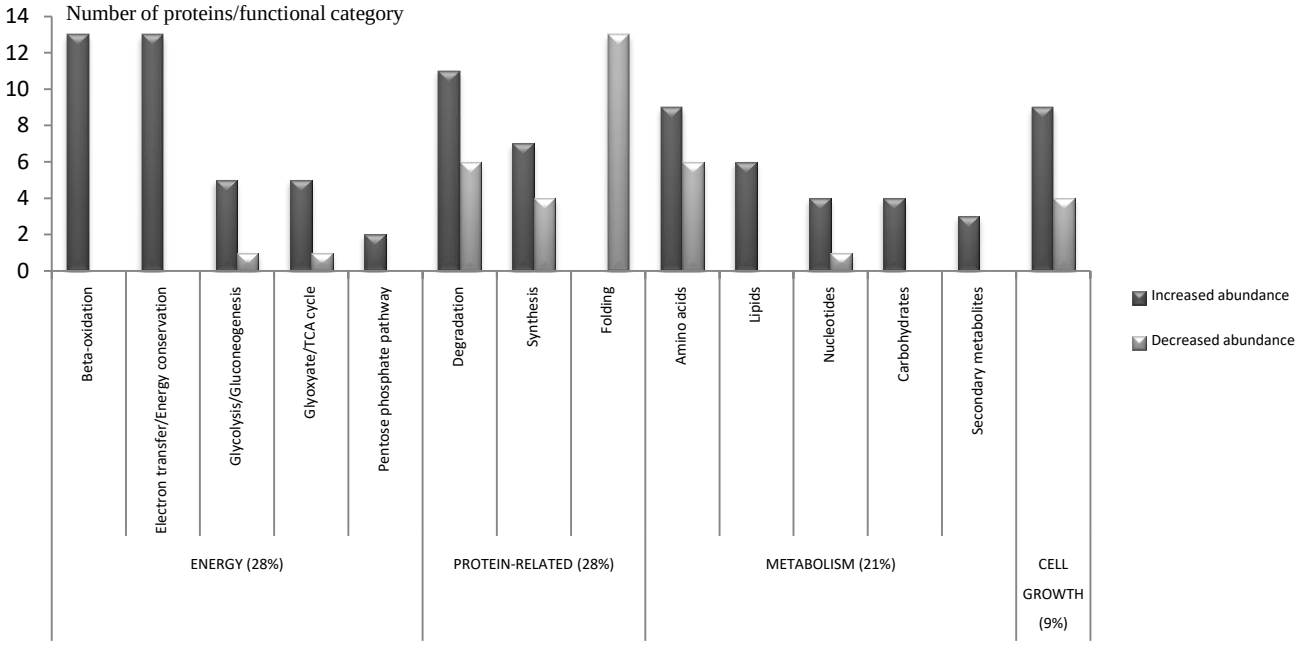
Number of proteins/functional category
14
12
10
8
6
4
2
0
Beta-oxidation
Electron transfer/Energy conservation
Glycolysis/Gluconeogenesis
Glyoxyate/TCA cycle
Pentose phosphate pathway
Degradation
Synthesis
Folding
Amino acids
Lipids
Nucleotides
Carbohydrates
Secondary metabolites
ENERGY (28%)
PROTEIN-RELATED (28%)
METABOLISM (21%)
CELL GROWTH (9%)
Increased abundance
Decreased abundance

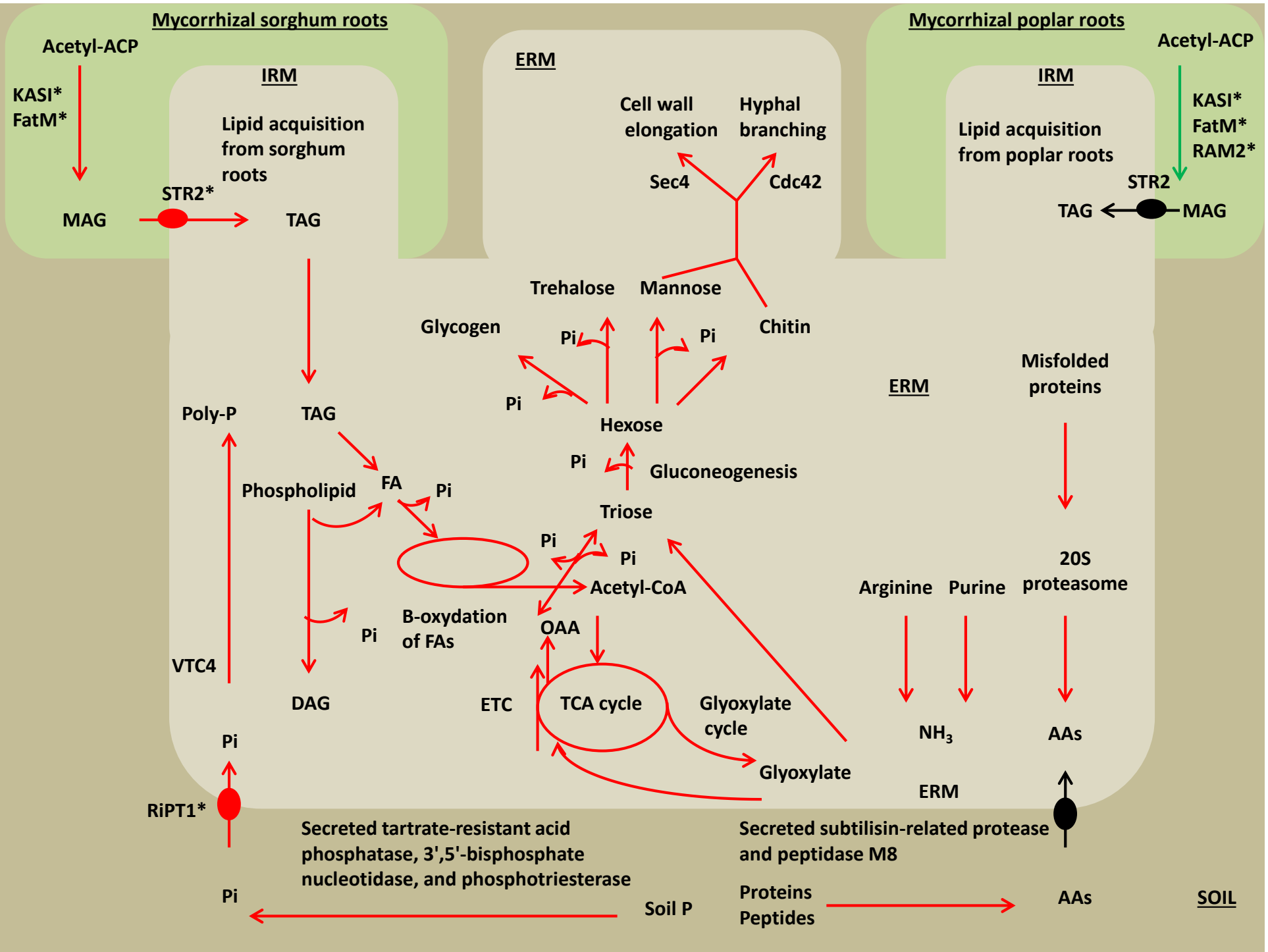
Mycorrhizal sorghum roots
Acetyl-ACP
KASI*
FatM*
MAG
IRM
Lipid acquisition from sorghum roots
STR2*
TAG
ERM
Cell wall elongation
Hyphal branching
Sec4
Cdc42
Trehalose
Mannose
Chitin
Glycogen
Pi
Pi
Pi
Hexose
Pi
Gluconeogenesis
Triose
Pi
Pi
Acetyl-CoA
Poly-P
TAG
FA
Pi
Phospholipid
B-oxydation of FAs
Pi
VTC4
DAG
OAA
ETC
TCA cycle
Glyoxylate cycle
Glyoxylate
Pi
RiPT1*
Pi
Secreted tartrate-resistant acid phosphatase, 3',5'-bisphosphate nucleotidase, and phosphotriesterase
Soil P
Mycorrhizal poplar roots
Acetyl-ACP
KASI*
FatM*
RAM2*
IRM
Lipid acquisition from poplar roots
STR2
TAG
MAG
ERM
Misfolded proteins
20S proteasome
Arginine
Purine
NH_3
AAs
ERM
Secreted subtilisin-related protease and peptidase M8
Proteins
Peptides
AAs
SOIL